Electromagnetic Field Distribution of Phase-sequence Orientation of a Double-Circuit Power Transmission Line Based on Finite Element Method

P. PAO-LA-OR*, A. ISARAMONGKOLRAK, and T. KULWORAWANICHPONG
Power System Research Unit, School of Electrical Engineering
Institute of Engineering, Suranaree University of Technology
111 University Avenue, Muang District, Nakhon Ratchasima, 30000
THAILAND
*Corresponding author: padej@sut.ac.th

Abstract: - This paper proposes a mathematical model of electric and magnetic fields caused by high voltage conductors of electric power transmission systems by using a set of second-order partial differential equations. This study has considered the effect of conductor phase-sequence orientation on electromagnetic fields emitted around a double-circuit, extra high-voltage, power transmission line. Five typically-used phase-sequence orientations in Thailand and one three-phase fault for 500-kV double-circuit transmission lines are examined. Computer-based simulation utilizing the two dimensional finite element method in the time harmonic mode, instructed in MATLAB programming environment with graphical representation for electric and magnetic field strength have been evaluated. The simulation results showed that the phase-sequence orientation is one among key factors to influence the electromagnetic field distribution around the transmission line.

Key-Words: - Phase-sequence, Electric Fields, Magnetic Fields, Finite Element Method (FEM), Transmission Line, Computer Simulation

1 Introduction

For decades, due to the increasing of electrical power demands in Thailand, Electricity Generating Authority of Thailand (EGAT) decides to enlarge transmission capacity by installing 500-kV extra high-voltage power transmission lines in both AC and DC. In the AC system, double-circuit transmission lines consist of six conductors running in parallel. Orientation of the six conductors results in electric and magnetic field distribution that may cause some serious harm to electronic equipment or living things. From literature, basic electromagnetic theory [1] or image theory [2] are widely used for electromagnetic field calculation in high voltage power transmission lines. Even the study by EPRI [3], the basic electromagnetic theory was employed to analyze electric field strength resulting from orientation of conductor phase-sequences. So far, there is no report on electric and magnetic field calculation in this scope by using Finite Element Method (FEM).

The FEM is one of the most popular numerical methods used for computer simulation. The key advantage of the FEM over other numerical methods in engineering applications is the ability to handle nonlinear, time-dependent and circular geometry problems. Therefore, this method is suitable for solving the problem involving electric and magnetic field effects around the transmission line caused by circular cross-section of high voltage conductors.

In this paper, 500-kV, double-circuit, extra high-voltage power transmission lines are studied with six conductor phase-sequence orientation. Computer-based simulation utilizing the two dimensional finite element method in the time harmonic mode, instructed in MATLAB programming environment with graphical representation for electric and magnetic field strength have been evaluated. In general, electric field strength of the system depends on operating voltage level applied to phase conductors. Due to the voltage regulation of the transmission systems, the conductor surface potential does not change to result in remarkable difference of the electric field contours. In the same manner, magnetic field strength of the system depends strongly on the phase currents flowing through the phase conductors. As mentioned where a normal steady-state operation is assumed, the current does not suddenly change its value. Therefore, both field distribution are quasi-static.

2 Modeling of Electric and Magnetic Fields involving Electric Power Transmission Lines

A mathematical model of electric fields (**E**) radiating around a transmission line is usually expressed in

the wave equation (Helmholtz's equation) as Eq.(1) [4-5] derived from Faraday's law.

$$\nabla^2\mathbf{E} - \sigma\mu\frac{\partial\mathbf{E}}{\partial t} - \varepsilon\mu\frac{\partial^2\mathbf{E}}{\partial t^2} = 0 \quad (1)$$

…, where ε is the dielectric permittivity of media, μ and σ are the magnetic permeability and the conductivity of conductors, respectively.

A mathematical model of magnetic fields (**B**) for transmission lines is performed in form of the magnetic field intensity (**H**), which related to the equation, $\mathbf{B} = \mu\mathbf{H}$. This model can be characterized by using the wave equation (Helmholtz's equation) as Eq.(2) [4-5] derived from the Ampere's law.

$$\nabla^2\mathbf{H} - \sigma\mu\frac{\partial\mathbf{H}}{\partial t} - \varepsilon\mu\frac{\partial^2\mathbf{H}}{\partial t^2} = 0 \quad (2)$$

Due to the similarity between Eq.(1) and Eq.(2), formulation of the FEM used for the magnetic field problems is mathematically the same. One can point out this similarity by replacing the electric field (**E**) with the magnetic field intensity (**H**).

This paper has considered the system governing by using the time harmonic mode and representing the electric field in complex form, $\mathbf{E} = Ee^{j\omega t}$ [6], therefore,

$$\frac{\partial\mathbf{E}}{\partial t} = j\omega E \quad \text{and} \quad \frac{\partial^2\mathbf{E}}{\partial t^2} = -\omega^2 E$$

…, where ω is the angular frequency.

From Eq.(1), by employing the complex form of the electric fields and assuming that the system is excited with a single frequency source, Eq.(1) can be transformed to an alternative form as follows.

$$\nabla^2 E - j\omega\sigma\mu E + \omega^2\varepsilon\mu E = 0$$

When considering the problem of two dimensions in Cartesian coordinate *(x,y)*, hence

$$\frac{\partial}{\partial x}\left(\frac{1}{\mu}\frac{\partial E}{\partial x}\right) + \frac{\partial}{\partial y}\left(\frac{1}{\mu}\frac{\partial E}{\partial y}\right) - \left(j\omega\sigma - \omega^2\varepsilon\right)E = 0 \quad (3)$$

Analytically, there is no simple exact solution of the above equation. Therefore, in this paper the FEM is chosen to be a potential tool for finding approximate electric field solutions for the PDE described in Eq.(3) [7-9].

3 System Description with the FEM

3.1 Discretization

This paper determines a four-bundled, double-circuit, 500-kV power transmission line. Fig. 1 shows the power transmission line with the low-reactance orientation type. Height of conductors shown in the figure is the maximum sag position. The lowest conductors are C and A′ at the height of 13.0 m above the ground level [10]. Each phase conductor is 795 MCM (0.02772 m - diameter). The overhead ground wire has 3/8 inch - diameter. Fig. 2 displays the domain of study discretizing by using linear triangular elements.

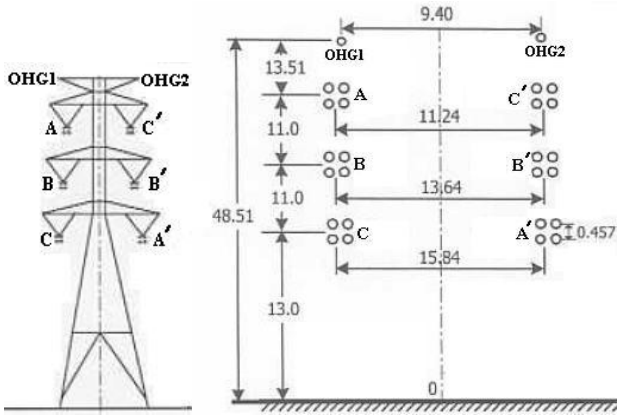

Fig.1 500-kV double-circuit, four-bundled power transmission line with low-reactance orientation

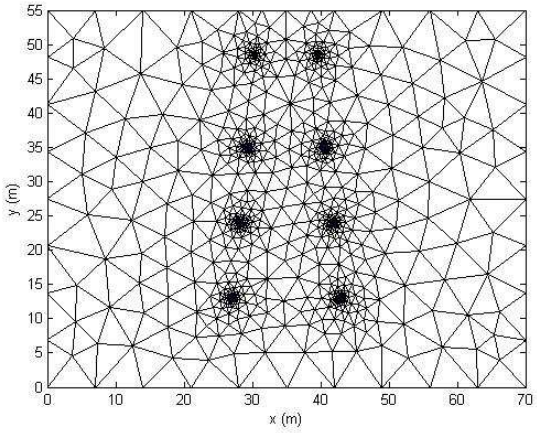

Fig.2 Discretization of the system given in Fig. 1

3.2 Finite Element Formulation

An equation governing each element is derived from the Maxwell's equations directly by using Galerkin approach, which is the particular weighted residual method for which the weighting functions are the

same as the shape functions [11-12]. According to the method, the electric field is expressed as follows.

$$E(x,y) = E_i N_i + E_j N_j + E_k N_k \quad (4)$$

…, where N_n , $n = i, j, k$ is the element shape function and the E_n , $n = i, j, k$ is the approximation of the electric field at each node (i, j ,k) of the elements, which is

$$N_n = \frac{a_n + b_n x + c_n y}{2\Delta_e}$$

…, where Δ_e is the area of the triangular element and,

$$a_i = x_j y_k - x_k y_j, \quad b_i = y_j - y_k, \quad c_i = x_k - x_j$$
$$a_j = x_k y_i - x_i y_k, \quad b_j = y_k - y_i, \quad c_j = x_i - x_k$$
$$a_k = x_i y_j - x_j y_i, \quad b_k = y_i - y_j, \quad c_k = x_j - x_i.$$

The method of the weighted residue with Galerkin approach is then applied to the differential equation, Eq.(3), where the integrations are performed over the element domain Ω.

$$\int_\Omega N_n \left(\frac{\partial}{\partial x}\left(\frac{1}{\mu}\frac{\partial E}{\partial x}\right) + \frac{\partial}{\partial y}\left(\frac{1}{\mu}\frac{\partial E}{\partial y}\right)\right) d\Omega - \int_\Omega N_n \left(j\omega\sigma - \omega^2\varepsilon\right) E \, d\Omega = 0$$

, or in the compact matrix form

$$[M + K]\{E\} = 0 \quad (5)$$

$$M = \left(j\omega\sigma - \omega^2\varepsilon\right)\iint_\Omega N_n N_m d\Omega = \frac{\left(j\omega\sigma - \omega^2\varepsilon\right)\Delta_e}{12}\begin{bmatrix} 2 & 1 & 1 \\ 1 & 2 & 1 \\ 1 & 1 & 2 \end{bmatrix}$$

$$K = \nu\int_\Omega \left(\frac{\partial N_n}{\partial x}\frac{\partial N_m}{\partial x} + \frac{\partial N_n}{\partial y}\frac{\partial N_m}{\partial y}\right) d\Omega = \frac{\nu}{4\Delta_e}\begin{bmatrix} b_i b_i + c_i c_i & b_i b_j + c_i c_j & b_i b_k + c_i c_k \\ & b_j b_j + c_j c_j & b_j b_k + c_j c_k \\ Sym & & b_k b_k + c_k c_k \end{bmatrix}$$

…, where ν is the material reluctivity ($\nu = 1/\mu$).

For one element containing 3 nodes, the expression of the FEM approximation is a 3×3 matrix. With the account of all elements in the system of n nodes, the system equation is sizable as the $n \times n$ matrix.

3.3 Boundary Conditions and Simulation Parameters

In this paper, 500-kV, double-circuit, extra high-voltage power transmission lines are studied with six conductor phase-sequence orientation [3] as shown in Table 1. The boundary conditions applied here are that both electric and magnetic fields at the ground level and the OHGW are set as zero. In contrast, the boundary conditions at the conductor surfaces are practically different. They are strongly dependent upon the load current for the magnetic case. However, in this paper, the boundary conditions of both electric and magnetic fields of conductor surfaces in 500-kV power lines are assigned as given in [3, 10, 13] under the maximum loading of 3.15 kA/phase [10]. This simulation uses the system frequency of 50 Hz. The power lines are bared conductors of Aluminum Conductor Steel Reinforced (ACSR), having the conductivity (σ) = 0.8×10^7 S/m, the relative permeability (μ_r) = 300, the relative permittivity (ε_r) = 3.5. It notes that the free space permeability (μ_0) is $4\pi\times10^{-7}$ H/m, and the free space permittivity (ε_0) is 8.854×10^{-12} F/m [14].

Table 1 Six cases of phase sequence orientation

type1	type2	type3	type4	type5	fault
A A′	A B′	A A′	A B′	A C′	A G
B B′	B A′	B C′	B C′	B B′	B G
C C′	C C′	C B′	C A′	C A′	C G

Notes for the table, letter A, B and C reserve for each phase of the first conductor circuit, whereas A′, B′ and C′ indicate those of the second circuit. G represents the ground potential (0 V).

4 Results and Discussion

This paper employs MATLAB programming to simulate electric field distribution for five typical phase-sequence orientations and one fault case. Electric field simulated for each type can be depicted in Fig. 3 – 8, respectively. Also, simulation results of magnetic field distribution for the six phase-sequence orientations can be shown in Fig. 9 – 14, respectively.

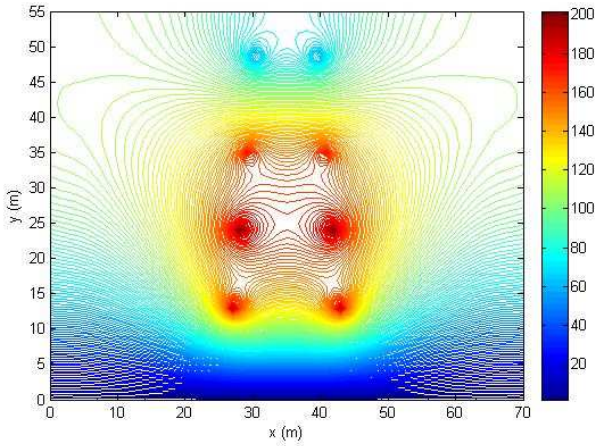

Fig.3 Electric field contour (kV/m) for type 1

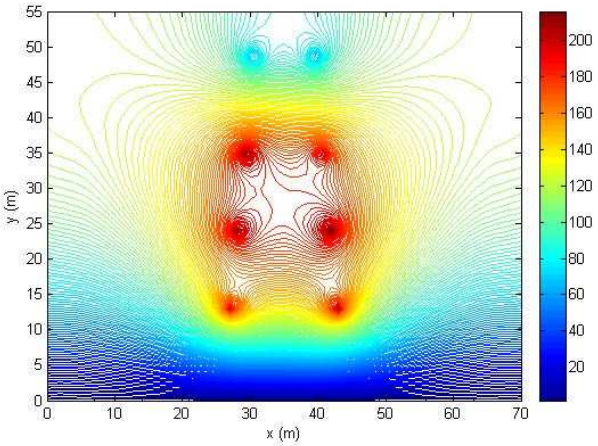

Fig.6 Electric field contour (kV/m) for type 4

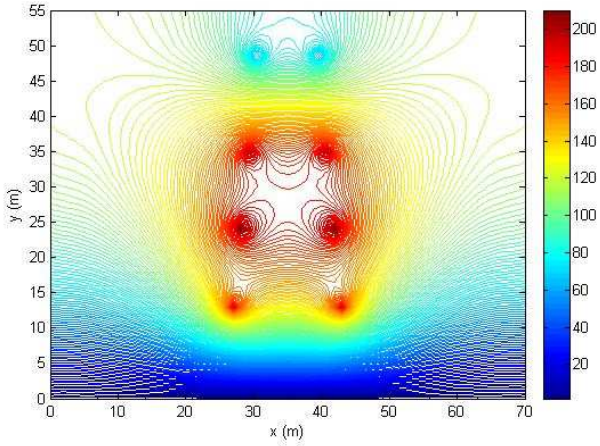

Fig.4 Electric field contour (kV/m) for type 2

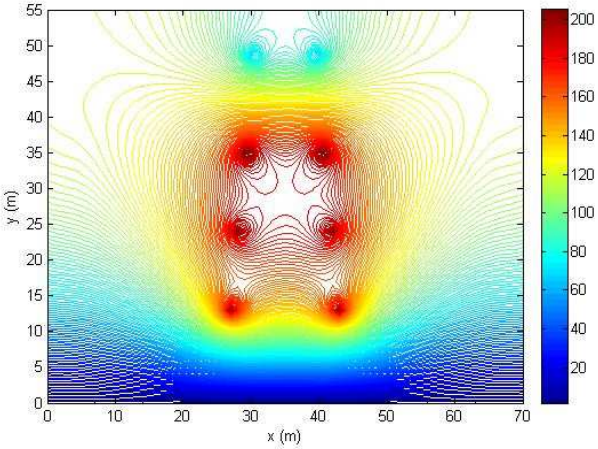

Fig.7 Electric field contour (kV/m) for type 5

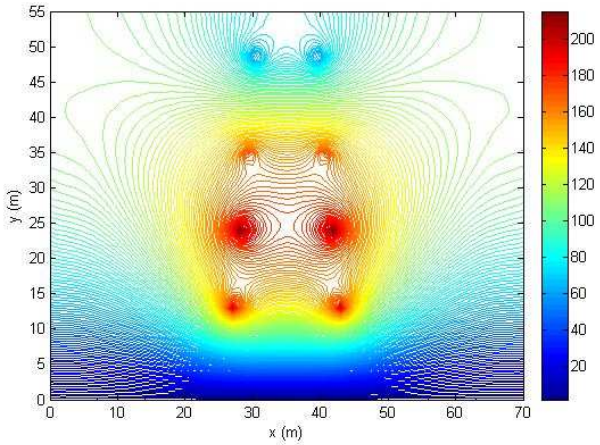

Fig.5 Electric field contour (kV/m) for type 3

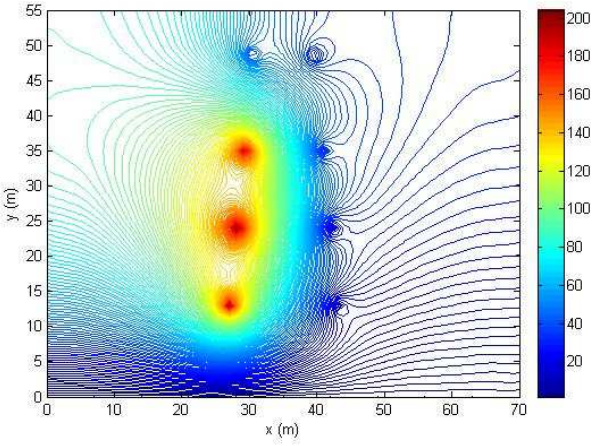

Fig.8 Electric field contour (kV/m) for the fault case

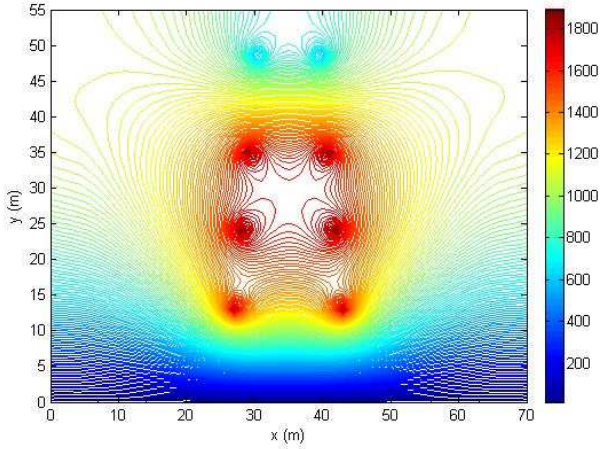

Fig.9 Magnetic field contour (μT) for type 1

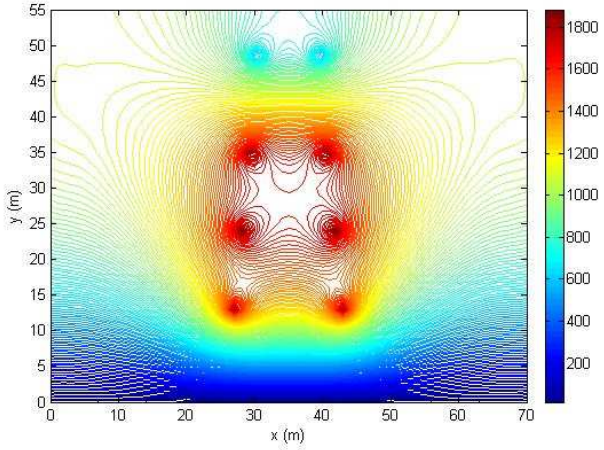

Fig.10 Magnetic field contour (μT) for type 2

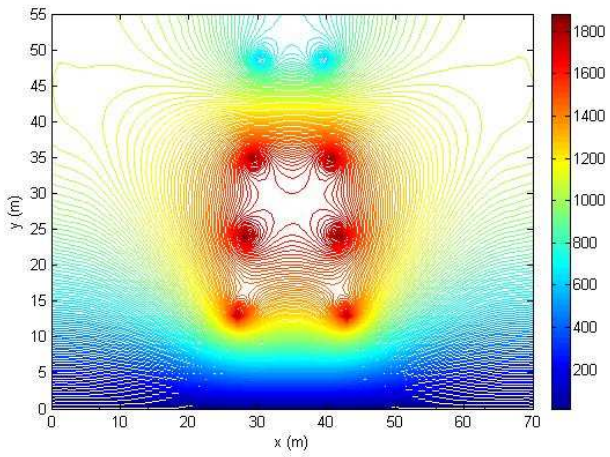

Fig.11 Magnetic field contour (μT) for type 3

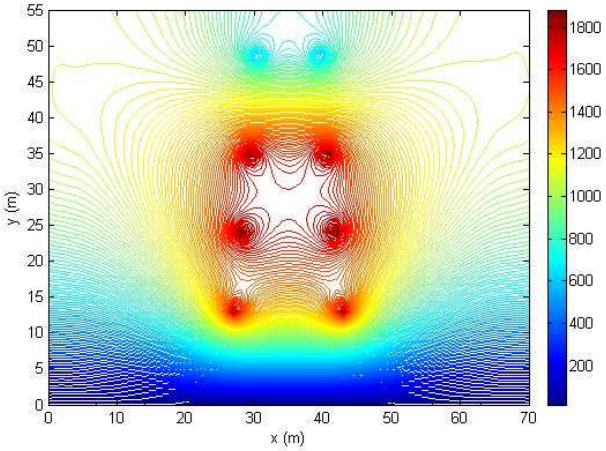

Fig.12 Magnetic field contour (μT) for type 4

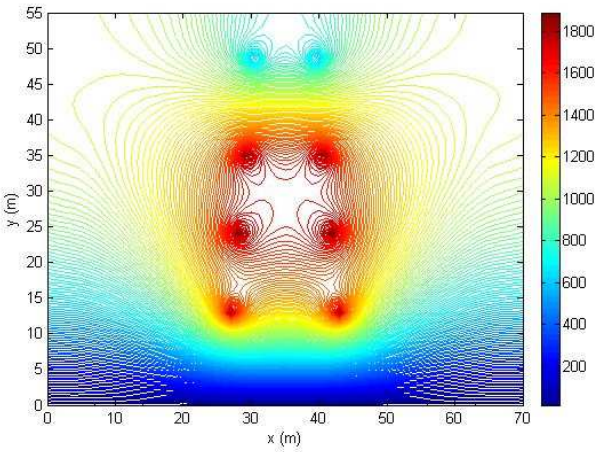

Fig.13 Magnetic field contour (μT) for type 5

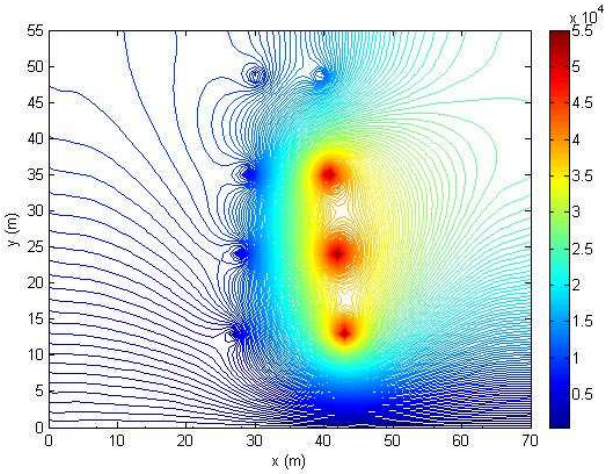

Fig.14 Magnetic field contour (μT) for the fault case

From the simulation results, the orientation type has the key effect on electric and magnetic field distribution around the power transmission line. By observing the electric field strength as shown in Fig. 3 – 8 at a specific height level above the ground with 70-m horizontal span, type 1, 2, 3 and 5 are symmetric in electric field distribution along the vertical axis. Type 4 and the fault are asymmetric due to unbalanced phase sequencing, especially type 6 with all the second circuit phases located on the right hand side shorted to ground as the three-phase fault occurred.

For the magnetic field cases as depicted in Fig. 9 – 14, except the fault case, all five typical phase orientations give symmetrically magnetic field distribution. Even in type 4, the magnetic field is also symmetric. It is because the magnetic flux lines are circular to enclose the conductor core, while the electric flux lines distribute perpendicularly from the conductor surfaces.

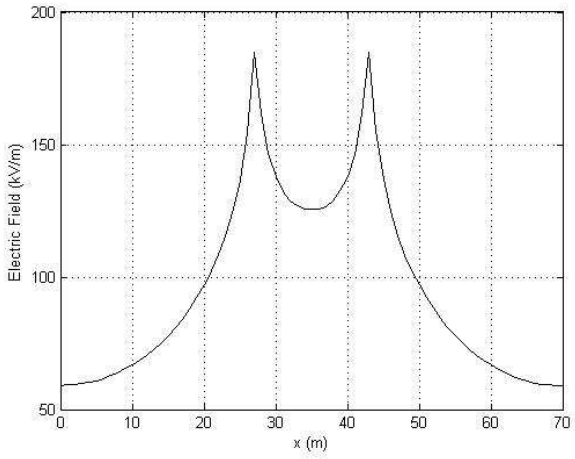

Fig.15 Electric field for type 1 at the height of 0.1 m below the lowest conductor position

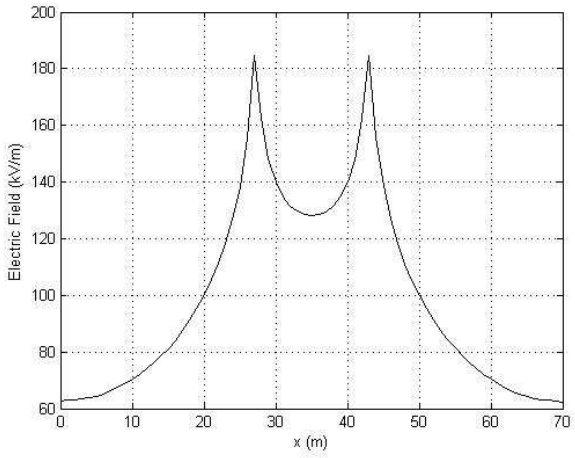

Fig.16 Electric field for type 2 at the height of 0.1 m below the lowest conductor position

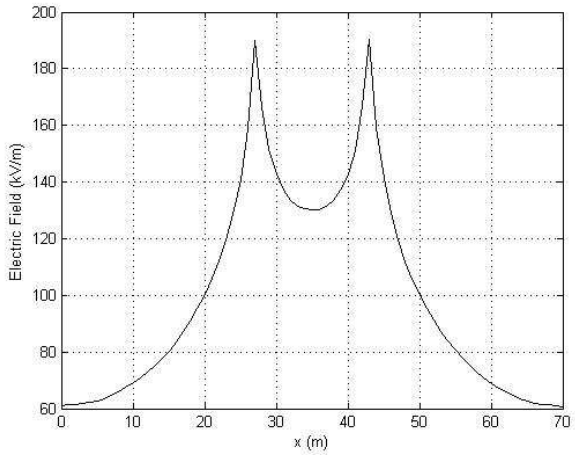

Fig.17 Electric field for type 3 at the height of 0.1 m below the lowest conductor position

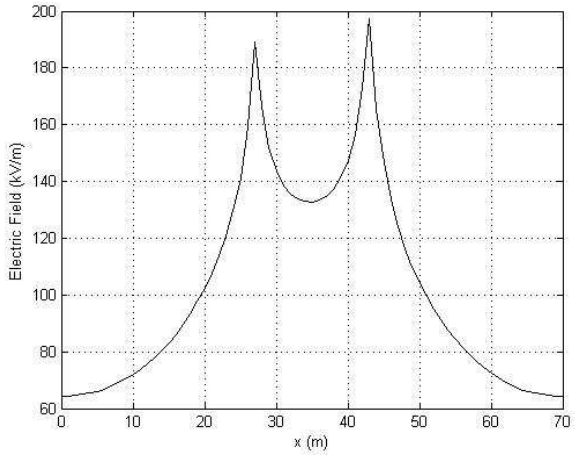

Fig.18 Electric field for type 4 at the height of 0.1 m below the lowest conductor position

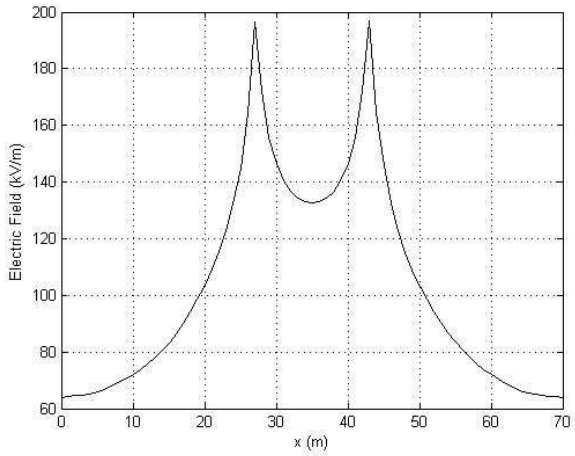

Fig.19 Electric field for type 5 at the height of 0.1 m below the lowest conductor position

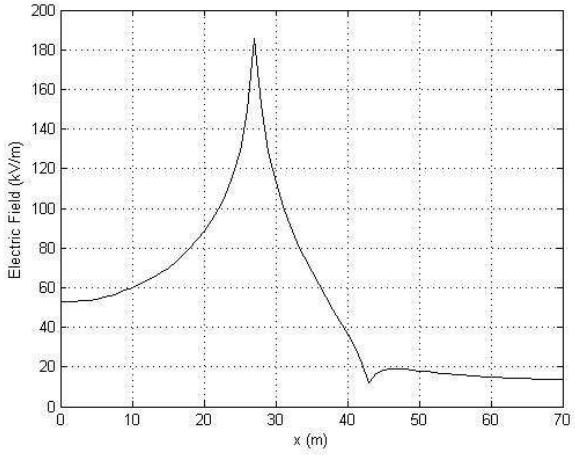

Fig.20 Electric field for the fault case at the height of 0.1 m below the lowest conductor position

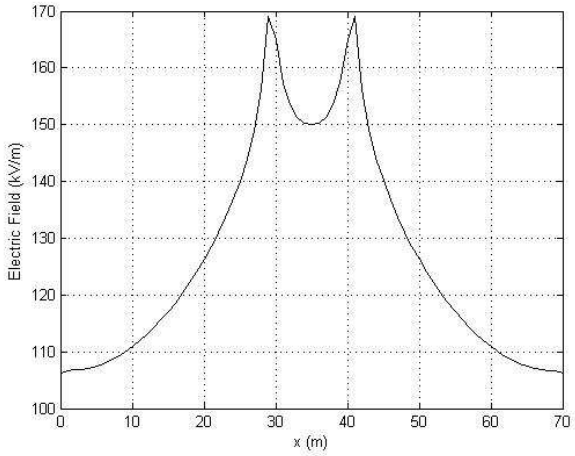

Fig.21 Electric field for type 1 at the height of 0.1 m above the highest conductor position

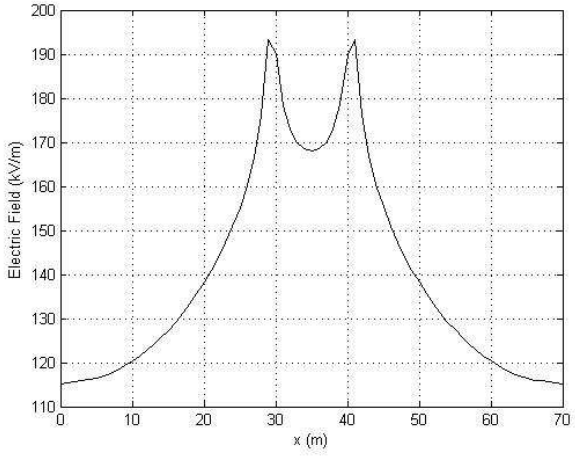

Fig.22 Electric field for type 2 at the height of 0.1 m above the highest conductor position

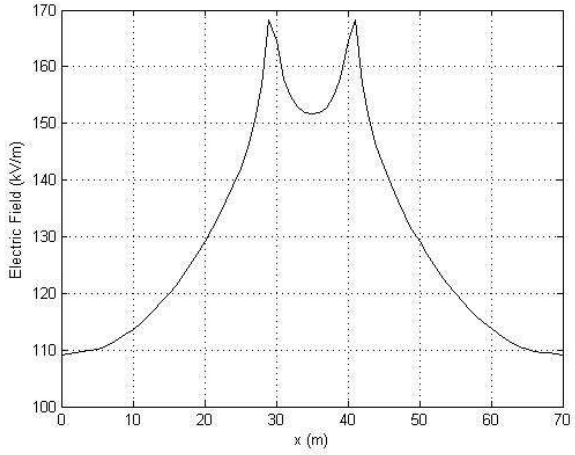

Fig.23 Electric field for type 3 at the height of 0.1 m above the highest conductor position

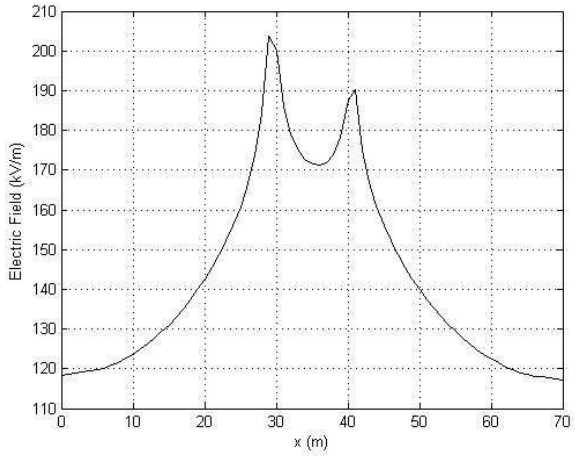

Fig.24 Electric field for type 4 at the height of 0.1 m above the highest conductor position

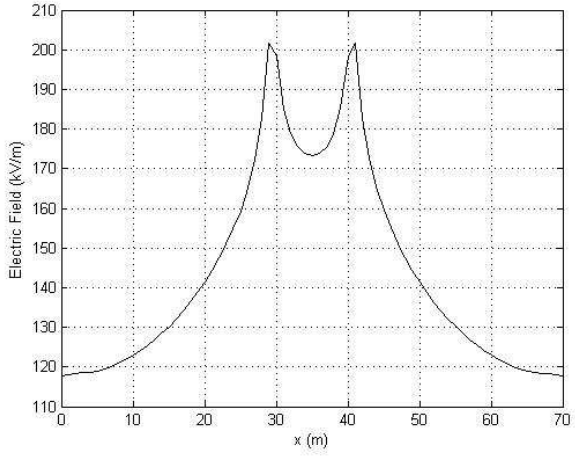

Fig.25 Electric field for type 5 at the height of 0.1 m above the highest conductor position

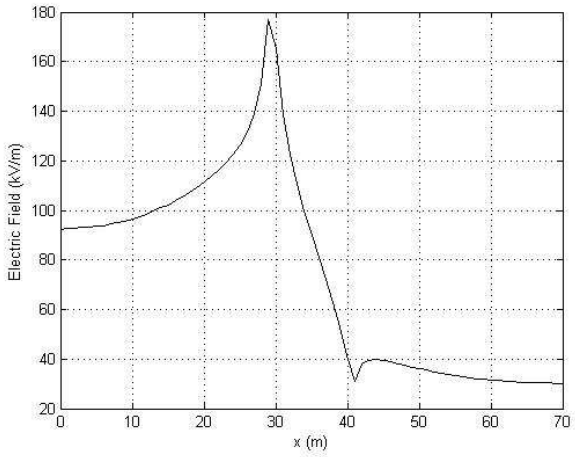

Fig.26 Electric field for the fault case at the height of 0.1 m above the highest conductor position

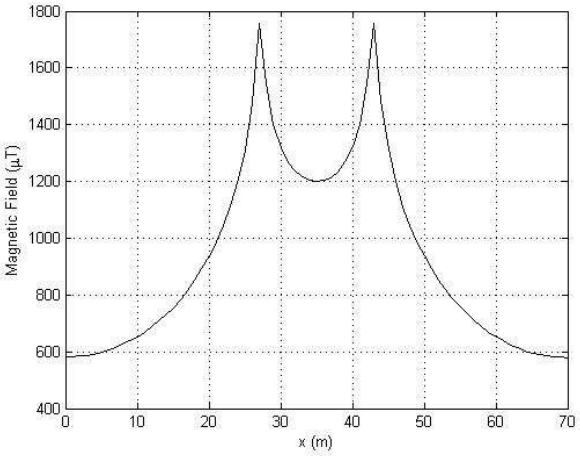

Fig.27 Magnetic field for type 1 at the height of 0.1 m below the lowest conductor position

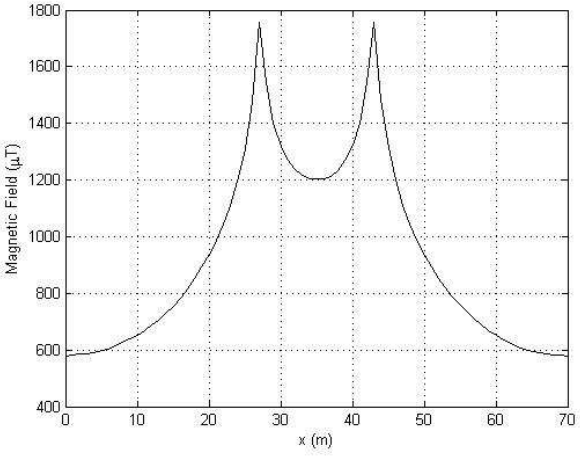

Fig.28 Magnetic field for type 2 at the height of 0.1 m below the lowest conductor position

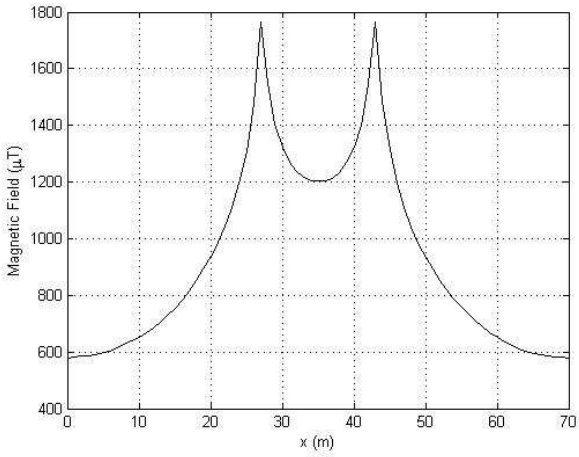

Fig.29 Magnetic field for type 3 at the height of 0.1 m below the lowest conductor position

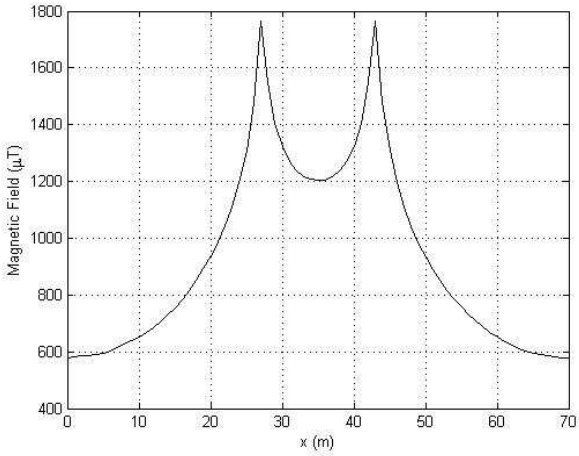

Fig.30 Magnetic field for type 4 at the height of 0.1 m below the lowest conductor position

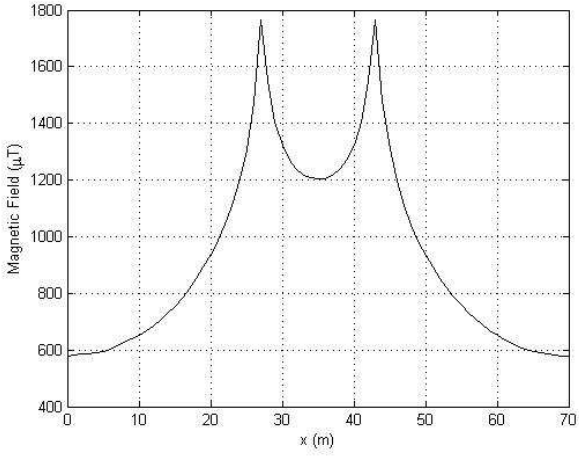

Fig.31 Magnetic field for type 5 at the height of 0.1 m below the lowest conductor position

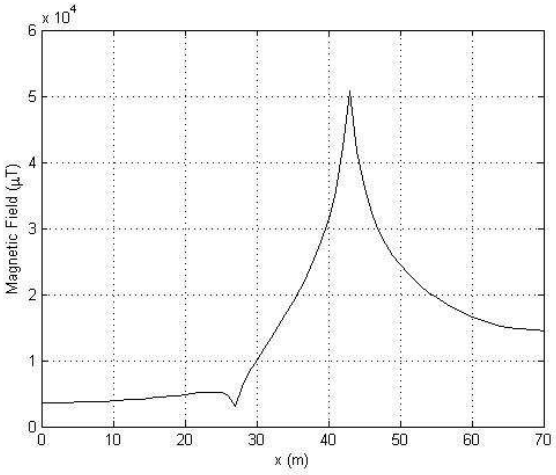

Fig.32 Magnetic field for the fault case at the height of 0.1 m below the lowest conductor position

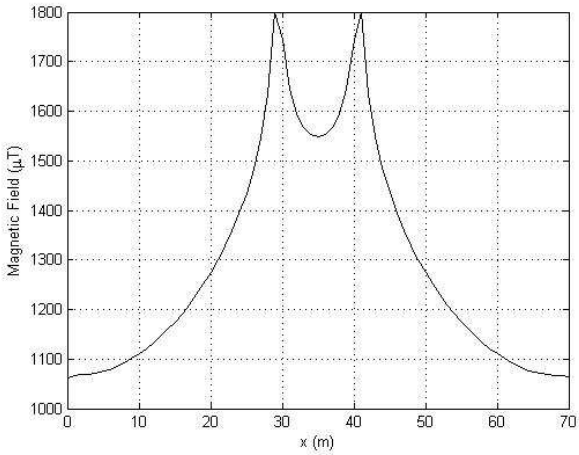

Fig.35 Magnetic field for type 3 at the height of 0.1 m above the highest conductor position

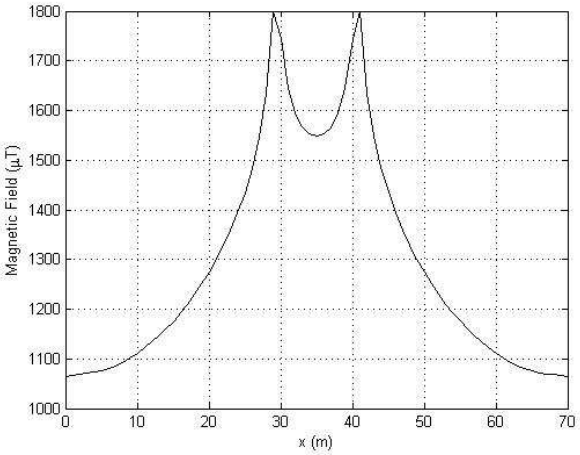

Fig.33 Magnetic field for type 1 at the height of 0.1 m above the highest conductor position

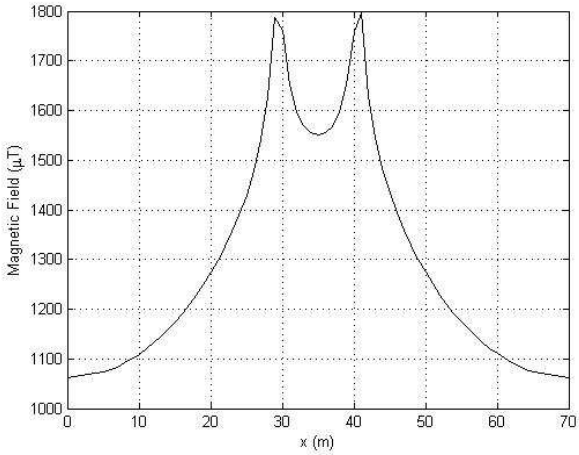

Fig.36 Magnetic field for type 4 at the height of 0.1 m above the highest conductor position

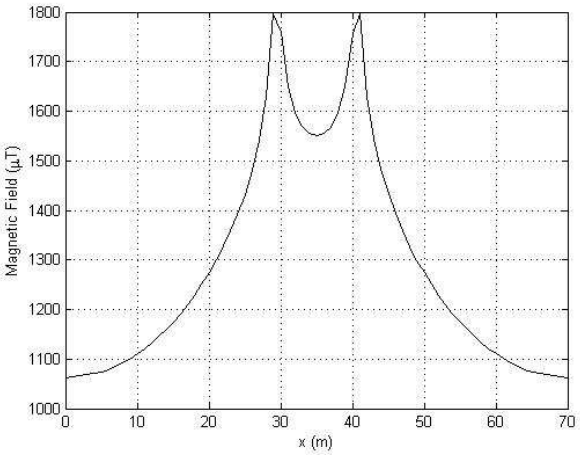

Fig.34 Magnetic field for type 2 at the height of 0.1 m above the highest conductor position

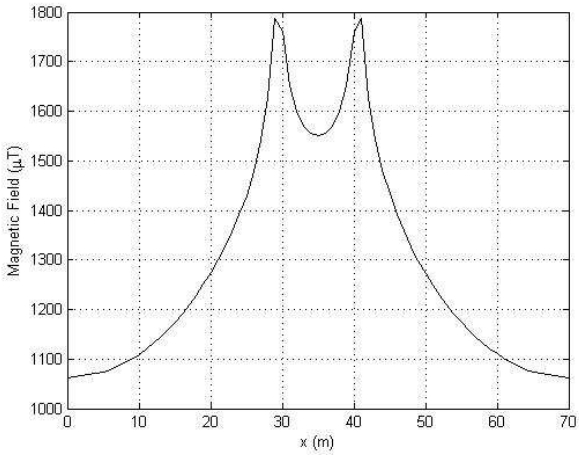

Fig.37 Magnetic field for type 5 at the height of 0.1 m above the highest conductor position

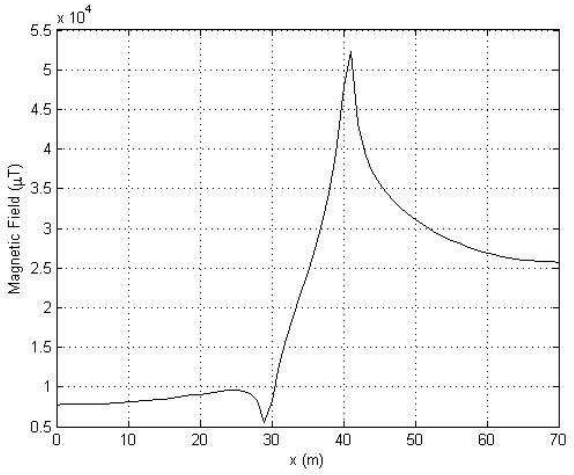

Fig.38 Magnetic field for the fault case at the height of 0.1 m above the highest conductor position

When consider at some selected positions for more detail, symmetry in electric field distribution can be clearly explained. Fig. 15 – 20 show the electric field plot at the height of 0.1 m below the lowest conductor position for each type. Similarly, Fig. 21 – 26 also describe the electric field plot at the height of 0.1 m above the highest conductor position for each type. They confirmed that type 1, 2, 3 and 5 are symmetric while type 4 and the fault are asymmetric as concluded by [3]. In addition, Fig. 27 – 32 show the magnetic field plot at the height of 0.1 m below the lowest conductor position for each type. Also, Fig. 33 – 38 also describe the magnetic field plot at the height of 0.1 m above the highest conductor position for each type.

5 Conclusion

This paper has studied electric and magnetic field distribution resulting from five typical conductor phase-sequence orientations and one three-phase fault case. 500-kV, double-circuit, four-bundled power transmission lines of Electricity Generating Authority of Thailand (EGAT) were investigated. FEM developed by using MATLAB programming was employed. As a result, phase-sequence orientation was one of key factors to influence electric and magnetic field distribution in electric power transmission lines. With the orientation of type 1, 2, 3 and 5, the electric field distribution was symmetric, while the left two cases (type 4 and the fault) gave asymmetric field distribution. For the magnetic field case, the orientation of type 1-5 gave the symmetrical magnetic field distribution, while the orientation of the fault case generated the asymmetric field distribution.

References:

[1] Olsen, R.G., Deno, D., Baishiki, R.S., Abbot, J.R., Conti, R., Frazier, M., Jaffa, K., Niles, G.B., Stewart, J.R., Wong, R., and Zavadil, R.M., Magnetic Fields from Electric Power Lines Theory and Comparison to Measurements, *IEEE Transactions on Power Delivery*, Vol.3, No.4, 1988, pp. 2127-2136.

[2] Li, L., and Yougang, G., Analysis of Magnetic Field Environment near High Voltage Transmission Lines, *Proceedings of the International Conferences on Communication Technology*, 1998, pp. S26-05-1 - S26-05-5.

[3] Electric Power Research Institute, *Transmission-Line Reference Book 345 kV and Above*, Fred Weidner & Son Printers, Inc., USA, 1975.

[4] Chari, M.V.K., and Salon, S.J., *Numerical Methods in Electromagnetism*, Academic Press, USA, 2000.

[5] Weiner, M., *Electromagnetic Analysis Using Transmission Line Variables*, World Scientific Publishing, Singapore, 2001.

[6] Christopoulos, C., *The Transmission-Line Modeling Method: TLM*, IEEE Press, USA, 1995.

[7] Pao-la-or, P., Kulworawanichpong, T., Sujitjorn, S., and Peaiyoung, S., Distributions of Flux and Electromagnetic Force in Induction Motors: A Finite Element Approach, *WSEAS Transactions on Systems*, Vol.5, No.3, 2006, pp. 617-624.

[8] Pao-la-or, P., Sujitjorn, S., Kulworawanichpong, T., and Peaiyoung, S., Studies of Mechanical Vibrations and Current Harmonics in Induction Motors Using Finite Element Method, *WSEAS Transactions on Systems*, Vol.7, No.3, 2008, pp. 195-202.

[9] Chen, R.C., An Iterative Method for Finite-Element Solutions of the Nonlinear Poisson-Boltzmann Equation, *WSEAS Transactions on Computers*, Vol.7, No.4, 2008, pp. 165-173.

[10] Pin-anong, P., *The Electromagnetic Field Effects Analysis which Interfere to Environment near the Overhead Transmission Lines and Case Study of Effects Reduction*, [M.Eng. thesis], School of Electrical Engineering, Department of Electrical Engineering, King Mongkut's Institute of Technology Ladkrabang, Bangkok, Thailand, 2002.

[11] Preston, T.W., Reece, A.B.J., and Sangha, P.S., Induction Motor Analysis by Time-Stepping Techniques, *IEEE Transactions on Magnetics*, Vol.24, No.1, 1988, pp. 471-474.

[12] Kim, B.T., Kwon, B.I., and Park, S.C., Reduction of Electromagnetic Force Harmonics in Asynchronous Traction Motor by Adapting

the Rotor Slot Number, *IEEE Transactions on Magnetics*, Vol.35, No.5, 1999, pp. 3742-3744.

[13] Iyyuni, G.B., and Sebo, S.A., Study of Transmission Line Magnetic Fields, *Proceedings of the Twenty-Second Annual North American, IEEE Power Symposium*, 1990, pp. 222-231.

[14] Hayt, Jr.W.H., and Buck, J.A., *Engineering Electromagnetics (7th edition)*, McGraw-Hill, Singapore, 2006.